

Superconducting properties of well-shaped MgB₂ single crystals

Kijoon H. P. Kim,* Jae-Hyuk Choi, C. U. Jung, P. Chowdhury, Hyun-Sook Lee, Min-Seok Park, Heon-Jung Kim, J. Y. Kim, Zhonglian Du, Eun-Mi Choi, Mun-Seog Kim, W. N. Kang, and Sung-Ik Lee

National Creative Research Initiative Center for Superconductivity and Department of Physics, Pohang University of Science and Technology, Pohang 790-784, Republic of Korea

Gun Yong Sung

Telecommunications Basic Research Laboratory, Electronics and Telecommunications Research Institute, Taejon 305-350, Republic of Korea

Jeong Yong Lee

Department of Material Science and Engineering, Korea Advanced Institute of Science and Technology, Taejon 305-701, Republic of Korea

(Received 26 November 2001; published 26 February 2002)

We report measurements of the transport and the magnetic properties of high-quality, sub-millimeter-sized MgB₂ single crystals with clear hexagonal-plate shapes. The low-field magnetization and the magnetic hysteresis curves show the bulk pinning of these crystals to be very weak. The Debye temperature of $\Theta_D \sim 1100$ K, obtained from the zero-field resistance curve, suggests that the normal-state transport properties are dominated by electron-phonon interactions. The resistivity ratio between 40 K and 300 K was about 5, and the upper critical field anisotropy ratio was 3.0 ± 0.2 at temperatures around 32 K.

DOI: 10.1103/PhysRevB.65.100510

PACS number(s): 74.70.Ad, 74.25.Bt, 74.25.Fy, 74.60.Ge

The recent discovery¹ of binary metallic MgB₂ with a superconducting transition temperature of 39 K has attracted great scientific^{2–20} and applicatory interests.^{21–26} The negligibly small effect of its grain boundary on the supercurrent^{21–23} suggests increased potential for device applications. Also, vortex pinning, and thus the critical current, is vastly enhanced in *c*-axis-oriented thin films^{24,25} or in the bulk when disorder is induced by proton irradiation.²⁶ Aside from basic properties such as the charge carrier type,² many scientific issues, such as the order parameter symmetry,^{3,4} the upper critical field anisotropy ratio,^{5,12} $\gamma = H_{c2}^{ab}/H_{c2}^c$, the Θ_D ,²⁷ and the transport properties of the normal state are still controversial.

Especially, the anisotropy is an important property because it significantly affects the electronic and the magnetic properties, such as the pinning mechanism of this material. The anisotropy ratio has been reported to be 6–9 for the powder. This range of values was estimated by using conduction electron spin resonance.²⁸ The values for aligned crystallites,⁵ *c*-axis oriented films,^{12,29} and single crystals grown by different techniques^{15,16} are reported to be 1.7, 1.3–2, and 2.6–2.7, respectively.

The high superconducting transition temperature in MgB₂ has been considered to be due to strong electron-phonon coupling.^{17,30,31} Thus, a very important question exists: can the normal-state transport properties be described by a simple electron-phonon interaction alone, or does electron correlation have to be taken into account?

Other issues are the temperature dependence of the normal-state resistivity and the value of the residual resistivity ratio (RRR), $\rho(300 \text{ K})/\rho(40 \text{ K})$. The RRR has been reported to vary from 2 to 25 depending on the preparation conditions,^{6–10,24,25} and the magnetoresistance (MR) of the

normal state has been reported to vary from 1% to 60%,^{8,10–12} with a rough correlation between higher RRR and higher MR values. These issues can be clarified if these quantities are measured in very clean single crystals. Such results will also help to construct a theoretical formulation.¹³

Here we report the transport and the magnetic properties of very clean MgB₂ single crystals. The crystals were found to have well-shaped hexagonal plates with an *a*-axis lattice constant of 3.09 Å. The superconducting transition occurred at 38 K with a sharp transition width of 0.3 K. The low-field magnetization and the magnetic hysteresis curve showed the bulk pinning to be very weak, which supported our crystals being very clean. The γ and the Θ_D were obtained by directly measuring the temperature and the field dependence of the resistance for different field directions.

MgB₂ bulk pieces^{8,14} were heat treated in a Mg flux inside a Nb tube, which was sealed in an inert gas atmosphere by using an arc furnace. Then, the Nb tube was put inside a quartz ampoule, which was sealed in a vacuum. The quartz tube was heated for one hour at 1050°C, then very slowly cooled to 700°C for five to fifteen days, and quenched to room temperature. For all measurements, the single crystals were separated from the resultant matrix by using a mechanical method. The details of growth can be found elsewhere.³² The crystal images were observed using a polarizing optical microscope and a field-emission scanning electron microscope (SEM). Structural analysis was carried out using a high-resolution transmission electron microscope (HRTEM). The magnetization curves were measured by using a superconducting quantum interference device (SQUID) magnetometer. Resistivity measurements were performed using the standard dc four-probe method.

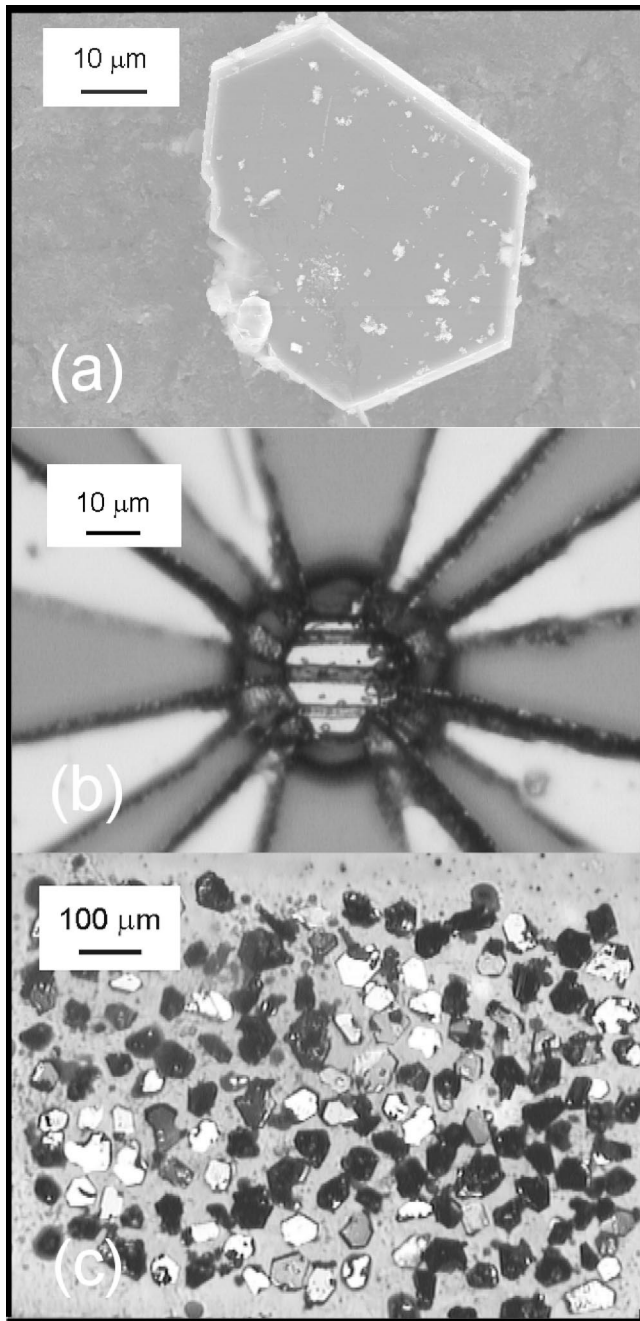


FIG. 1. (a) SEM image of a hexagonal, thin plate with a size of about $50 \mu\text{m}$, shows smooth surfaces and sharp edges. The white spots at the edge were stuck weakly on the crystal surface and were about 100 nm in diameter. (b) Optical microscope image of the four-probe contact leads which were made on a single crystal by using a photolithography technique. (c) Two hundred single crystals on a Si substrate with their c axes aligned perpendicular to the substrate surface within $\pm 2.5^\circ$.

Figure 1(a) shows a typical SEM image for a MgB_2 single crystal. Most of the crystals were found to have hexagonal-plate forms with typical edge angles of 120 degrees and with very flat surfaces, which were very shiny when observed using a polarizing optical microscope. The crystals were about $20\text{--}120 \mu\text{m}$ in diagonal length and $2\text{--}10 \mu\text{m}$ in

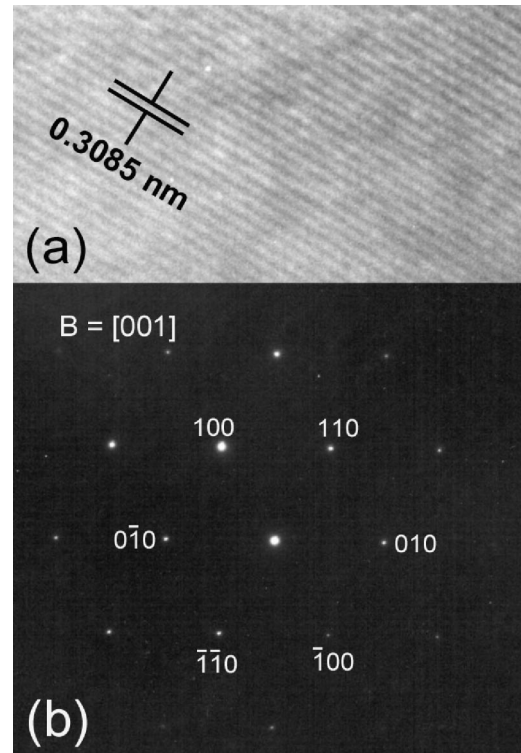


FIG. 2. (a) HRTEM image of a MgB_2 single crystal and (b) selected area electron diffraction pattern for a beam direction of $[001]$ in the hexagonal structure.

thickness. A recent study⁶ showed that $[001]$ twist grain boundaries, formed by rotations along the c axis (typically by about 4 degrees), were the major grain boundaries in polycrystalline MgB_2 and could be attributed to the weaker Mg-B bonding.⁶ HRTEM and SEM studies showed no grain boundaries in our crystals. The smooth surfaces and the sharp edges confirm that our small crystals had the least probability of having mosaic aggregates of nanocrystals either along the ab plane or along the c axis; thus, we had a better chance to study their intrinsic properties with the help of a microfabrication technique.

To measure the temperature and the field dependencies of the in-plane resistivity of the crystal, we fabricated four electrical metal leads (bright area) on the top surface of the crystal, as shown in Fig. 1(b). For lithography, selected MgB_2 single crystals were fixed on oxidized Si substrate by holding their hexagonal edges using a negative photoresist (OMR-83, TOK Co. Ltd.) as glue. They were then soft baked. After the surfaces of the samples were cleaned by using Ar-ion milling with a beam voltage of 350 V and a beam current of 0.2 mA/cm^2 , four electrical pads were patterned using a positive photoresist (AZ 7210, Clariant Industries Ltd.). Three metal layers, a 100-nm thick Ti film, a 1000-nm thick Ag film, and a 100-nm -thick Au film, were deposited in sequence after another ion milling treatment. The contact resistances were less than 2Ω , and the approximate distance between the voltage pads was about $7 \mu\text{m}$. The bias current for the resistance measurement was $0.1\text{--}0.2 \text{ mA}$, which, judging from the current-voltage characteristics, was in the ohmic range.

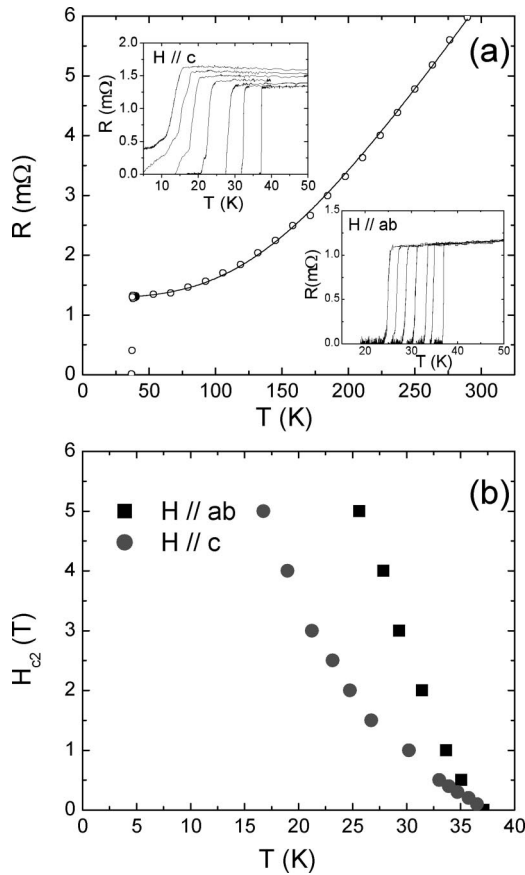


FIG. 3. (a) Resistance of a MgB_2 single crystal as a function of temperature for magnetic fields from 0 to 5 T. The residual resistivity ratio is about 5. The insets show the resistance for fields of 0.0, 0.5, 1.0, 2.0, 3.0, 4.0, and 5 T both perpendicular and parallel to the crystal c axis. (b) The upper critical field determined from a 10% drop of the resistance as a function of the temperature for several fields up to $H=5$ T.

For the bulk properties of the superconductivity, we measured the low-field magnetization curve $M(T)$ and the magnetic hysteresis curve $M(H)$. Since the volume of one crystal was rather small, we fixed about two hundred single crystals on a Si substrate with their c axes aligned perpendicular to the substrate surface within $\pm 2.5^\circ$ as shown in Fig. 1(c). To avoid spurious signals from the matrix, we used an optical microscope and a sample-handling device equipped with a precision xyz stage and a microtip to collect large single crystals one by one.

To confirm the structure of the MgB_2 phase, we took a plane-view HRTEM image, as shown in Fig. 2. From this high-resolution image, the a -axis lattice parameter was found to be 3.09 ± 0.06 Å, which was consistent with the value determined from x-ray powder diffractometry performed on polycrystalline samples.¹ Figure 2(b) shows the electron diffraction pattern in a selected area for a beam direction of [001]. This result clearly indicates that this crystal has the hexagonal structure of MgB_2 .

Figure 3(a) shows the in-plane resistance as a function of temperature. A superconducting transition appears near 38 K with a transition width of 0.3 K based on the 10 to 90% drop

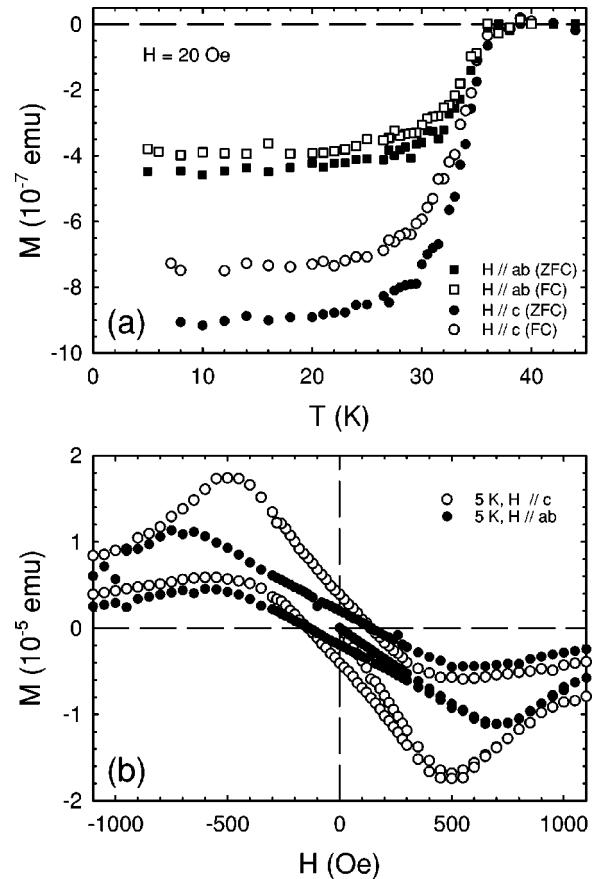


FIG. 4. (a) Low-field $M(T)$ curves of MgB_2 single crystals measured at 20 Oe for fields parallel and perpendicular to the c axis. (b) $M(H)$ hysteresis curves measured at 5 K.

of the resistance curve at zero field. The RRR is about 5, which was confirmed for several of our crystals and is consistent with the values recently reported for single crystals.^{15,16} This is quite different from the reported values for polycrystals^{6–10} and for high-quality thin films.^{24,25} Extrinsic effects, such as impurities or grain boundaries, might be the origins of these diverse observations.^{6,7} The c axis resistivity of single crystals should be studied in order to obtain a better understanding; however, this is still challenging due to the thickness of our crystals.

The solid line in Fig. 3 is a fitting curve obtained using the Bloch-Grüneisen formula²⁷ in the normal state: $R(T) = R_0 + R_{\text{ph}}(T)$ where R_0 is the temperature-independent residual part and $R_{\text{ph}}(T)$ the phonon scattering contribution given by the relation:

$$R_{\text{ph}}(T) = R_1 \left(\frac{T}{\Theta_D} \right)^m \int_0^{\Theta_D/T} \frac{z^m dz}{(1 - e^{-z})(e^z - 1)}, \quad (1)$$

with R_1 being a proportionality constant. The best fit to our data was obtained with $m=3.0$ and $\Theta_D \sim 1100$ K. This values of the Θ_D is comparable to those (746-1050 K) previously reported based on the specific heat and resistivity measurements on polycrystalline samples.^{17,18,33–35} This result suggests that the normal-state transport properties are well

described by an electron-phonon interaction without taking an electron-electron interaction into account.

The two insets of Fig. 3(a) show the field dependencies of the in-plane resistances while maintaining the applied field perpendicular to the current path. The magnetoresistance at 5 T was found to change with the direction of the field with respect to the crystal axis. For fields parallel to the ab -plane ($H\parallel ab$) and to the c axis ($H\parallel c$), the magnetoresistances at 40 K were $\approx 3\%$ and $\sim 20\%$, respectively, which was confirmed for several of our crystals. To determine the temperature dependence of the upper critical field H_{c2} , we measured the resistance at several fields up to 5 T. From these curves, we obtained $H_{c2}(T)$ as shown in Fig. 3(b), where a 10% drop of the resistance was adopted to determine $T_c(H)$. The ratio of the upper critical field for $H\parallel ab$ to that for $H\parallel c$ was 3.0 ± 0.2 at temperatures around 32 K. This value is consistent with those for single crystals grown by different techniques.^{15,16}

Figure 4(a) shows the $M(T)$ curves measured at 20 Oe in the zero-field-cooling (ZFC) and the field-cooling (FC) modes. The T_c onset was observed to be ~ 38 K, which is consistent with the value obtained from the resistance measurement. The difference between the FC and the ZFC data is quite small compared to those for polycrystalline samples^{8,14} and for single crystals prepared at higher temperature,¹⁶ suggesting that pinning is very weak in our single crystals. The different values of $M(T)$ for different field directions give a demagnetization factor $D \geq 0.6$, which is consistent with the value calculated by considering the shape of the crystals.

Figure 4(b) shows the magnetic hysteresis curves $M(H)$ at 5 K. The $M(H)$ data show a negligible paramagnetic

background, which is quite different from the case reported by de Lima *et al.*⁵ There are two notable features in the magnetic hysteresis curves. One is an asymmetry between the ascending and the descending branches, which has been not observed in bulk pinning dominated polycrystals^{19,20} and thin films.^{24,25} The other is the fact that the $J_c(H)$ is not a monotonically decreasing function of the magnetic field. The value of J_c , as estimated by using the Bean model,³⁶ has a maximum of $\sim 1.5 \times 10^5$ A/cm² at $H \sim 500$ Oe. The first behavior can be explained by surface pinning in very clean samples, not by the strong extrinsic pinning sites, such as grain boundaries and crystallographic defects.³⁷

In summary, we report the transport and the magnetic properties for high-quality MgB₂ single crystals. A superconducting transition occurred at 38 K with a sharp transition width of 0.3 K. The low-field magnetization and the magnetic hysteresis curve showed the bulk pinning to be very weak. From the resistance measurement, a Θ_D of ~ 1100 K was obtained using the Bloch-Grüneisen formula, which suggested that the normal-state transport properties were dominated by an electron-phonon interaction rather than by an electron-electron interaction. A RRR of 5 and a γ of 3.0 ± 0.2 at temperatures around 32 K were obtained.

This work was supported by the Ministry of Science and Technology of Korea through the Creative Research Initiative Program. This work was partially supported by the National Research Laboratory Program through the Korea Institute of Science and Technology Evaluation and Planning. We acknowledge Do Hyun Lim and Taek-Jung Shin at Iljin Diamond Co., Ltd., for their help.

*Email address : kijoon@phys.postech.ac.kr URL: <http://www-psc.postech.ac.kr>

¹J. Nagamatsu *et al.*, Nature (London) **410**, 63 (2001).

²W.N. Kang *et al.*, Appl. Phys. Lett. **79**, 982 (2001).

³P. Seneor *et al.*, Phys. Rev. B **65**, 012505 (2001).

⁴G. Karapetrov *et al.*, Phys. Rev. Lett. **86**, 4374 (2001).

⁵O.F. de Lima *et al.*, Phys. Rev. Lett. **86**, 5974 (2001).

⁶Y. Zhu *et al.*, cond-mat/6105311 (unpublished).

⁷Y.Y. Xue *et al.*, cond-mat/0145478 (unpublished).

⁸C.U. Jung *et al.*, Physica C **353**, 162 (2001).

⁹P.C. Canfield *et al.*, Phys. Rev. Lett. **86**, 2423 (2001).

¹⁰D.K. Finnemore *et al.*, Phys. Rev. Lett. **86**, 2420 (2001).

¹¹S.L. Bud'ko *et al.*, Phys. Rev. B **63**, 220503 (2001).

¹²M.H. Jung *et al.*, Chem. Phys. Lett. **343**, 447 (2001).

¹³Y. Kong *et al.*, Phys. Rev. B **64**, 020501 (2001).

¹⁴C.U. Jung *et al.*, Appl. Phys. Lett. **78**, 4157 (2001).

¹⁵M. Xu *et al.*, Appl. Phys. Lett. **79**, 2779 (2001).

¹⁶S. Lee *et al.*, J. Phys. Soc. Jpn. **70**, 2255 (2001).

¹⁷S.L. Bud'ko *et al.*, Phys. Rev. Lett. **86**, 1877 (2001).

¹⁸Ch. Wälti *et al.*, Phys. Rev. B **64**, 172515 (2001).

¹⁹M.-S. Kim *et al.*, Phys. Rev. B **64**, 012511 (2001).

²⁰Y. Takano *et al.*, Appl. Phys. Lett. **78**, 2914 (2001).

²¹Y. Bugoslavsky *et al.*, Nature (London) **410**, 563 (2001).

²²D.C. Labalestier *et al.*, Nature (London) **410**, 186 (2001).

²³K.H.P. Kim *et al.*, cond-mat/0103176 (unpublished).

²⁴W.N. Kang *et al.*, Science **292**, 1523 (2001).

²⁵C.B. Eom *et al.*, Nature (London) **411**, 558 (2001).

²⁶Y. Bugoslavsky *et al.*, Nature (London) **411**, 561 (2001).

²⁷Charles P. Poole, Jr., *Handbook of Superconductivity* (Academic Press, Florida, 2000), pp. 31,32.

²⁸F. Simon *et al.*, Phys. Rev. Lett. **87**, 047002 (2001).

²⁹S. Patnaik *et al.*, Supercond. Sci. Technol. **14**, 315 (2001).

³⁰J. Kortus *et al.*, Phys. Rev. Lett. **86**, 4656 (2001).

³¹M. Monteverde *et al.*, Science **292**, 75 (2001).

³²C.U. Jung *et al.* (unpublished) or Jae-Hyuk Choi, Ph.D. dissertation, Postech, Korea, 2001.

³³R.K. Kremer *et al.*, cond-mat/0102432 (unpublished).

³⁴F. Bouquet *et al.*, Phys. Rev. Lett. **87**, 047001 (2001).

³⁵M. Putti *et al.*, cond-mat/0106344 (unpublished).

³⁶C.P. Bean, Phys. Rev. Lett. **8**, 250 (1962).

³⁷M. Pissas *et al.*, cond-mat/0108513 (unpublished).